A methodology to account for local geology at large scale in the SHA approach through numerical modelling of theoretical geological sections

D. Di Bucci[1], G. Naso[1], S. Marcucci[1], G. Milana[2] and T. Sanò[3]

[1] *Dipartimento della Protezione Civile, Servizio Sismico Nazionale, Rome, Italy*
[2] *Istituto Nazionale di Geofisica e Vulcanologia, Rome, Italy*
[3] *Consultant of the Dipartimento della Protezione Civile, Servizio Sismico Nazionale, Rome, Italy*

(Received October 9, 2002; accepted September 28, 2004)

ABSTRACT Local geology in the standard procedure of Seismic Hazard Assessment (SHA), at national scale, is not taken into account nowadays. Microzonation studies are very expensive and time consuming for an extensive application to regional territories, while quick and simplified methods could help in this context. Therefore, in the present paper an innovative simplified approach is proposed, aimed at quickly collecting information on the local geology of small towns and villages in order to define a first estimate of the geological contribution to the bedrock-referred SHA.
We defined a set of ten 1D and 2D geological and morphological settings, represented by schematic cross-sections that characterise most of the Italian small towns and villages, along with six lithotype classes defined on the basis of their shear wave velocity. These sections were numerically modelled, to include also nonlinear effects. Response spectra and amplification factors were calculated for three different kinds of seismic input at the bedrock. In order to apply the results obtained to large parts of the Italian territory, and possibly integrate them in the seismic hazard maps, Italian municipalities' technicians were asked to classify their small towns or villages on the basis of geological settings here presented by filling in a form. These data, organised in a database and a GIS, will make it possible to associate the results of the numerical modelling to every Italian small municipality. In this way, the amplification factor values obtained could contribute to the definition of a first estimate of the role played by the local geology to bedrock-referred SHA at a large scale.

1. Introduction

The seismic hazard maps of Italy (Romeo and Pugliese, 1998; Slejko *et al.*, 1998; Albarello *et al.*, 2000) presently available for the national territory do not take into account the effects induced on the ground motion by the geological setting of the sites.

Romeo *et al.* (2000), working at a 1:500,000 scale, made a first attempt to consider at least the contribution of the lithology. However, that scale did not allow a good definition of the local geology, especially for the small towns and villages; therefore, the study of Romeo *et al.* (2000) did not take into account morphological and 2D geological settings.

Actually, only a microzonation study could provide an accurate geological definition of each site, able to contribute to the Seismic Hazard Assessment (SHA). On the other hand,

microzonation studies are very expensive and time consuming for an extensive application to regional territories, while quick and simplified methods could help in this context. Therefore, in the present paper an innovative simplified approach is proposed, aimed at quickly collecting information on the local geology of small towns and villages in order to define a first estimate of the geological contribution to the bedrock-referred SHA.

The methodology is divided into the following steps:

1) a table of lithotypes grouped in six S wave velocity classes was defined;
2) ten schematic 2D geological and morphological sections were realised; rocks of these sections refer to the table of lithotypes;
3) municipality technicians were asked to classify Italian small towns and villages by filling in a form containing the table of lithotypes and the schematic geological sections;
4) these data were organised into a database and in a GIS;
5) three seismic input energy levels were chosen;
6) numerical modelling was performed by applying 1D and 2D computer codes to the schematic geological sections; this returned mean response spectra and amplification factors (*AFs*) for each case modelled;
7) the consistency of the obtained results with microzonation analysis for realistic cases was evaluated;
8) the aforementioned database and GIS allow the results of numerical modelling to be associated to small Italian municipalities;
9) these AF values obtained could represent a preliminary attempt to consider the local geology contribution in the hazard maps at large scale.

This simplified approach is based on the following main assumptions:

a) the methodology is designed for a possible application to hazard maps at large scale (1:100,000 and over); this implies that:
   - the *AF* obtained for each site are applied to the related municipality territory as a whole;
   - the results are expressed as both acceleration response spectra (function of the period) and mean values of velocity response spectra (in prescribed period ranges);
   - coseismic effects such as landslides, liquefaction, surface faulting and tsunamis are not considered;
   - the interaction field-anthropic structures are neglected;
b) a realistic schematization of the local geological setting is needed; this implies that:
   - the number of possible geological schemes is high;
   - these schemes are based on 2D geological cross-sections;
   - a velocity gradient is used as function of the depth;
   - non-linearity functions are applied;
   - the chosen seismic energy level varies as function of the seismicity known for each site;
c) the degree of detail of the geological information has to be calibrated for the possible integration of the results in large scale hazard maps; this implies that:
   - the parameters that describe the geological schemes (*Vs*, thickness, slope dip, etc.) are characterised by realistic yet mean range values;
   - the extreme cases, even if real, are not considered;

- as each site is classified with only one (rarely two) geological scheme, this methodology can be applied only to small municipalities;
- modelling results, that treat the local geology in correspondence with small towns or villages, are applied to the entire municipalities' territory;
- the analyses refer to shear modulus and damping relationships currently applied and well-known from the literature;
- the three energy levels applied represent mean seismic inputs;

d) this methodology cannot be referred to as a microzonation; this implies that:
- the results presented (*AF* values) cannot be regarded as reference values at a local scale;
- the methodology cannot be applied for local planning and designing purposes.

Summing up, this work allowed the identification of geological settings that predispose a site to greater or lesser levels of shaking, and *AF* mean values have been obtained for these settings. The degree of detail is calibrated for a possible integration of the results obtained in large scale hazard maps. As in these maps the hazard values are referred to the entire area of each municipality, our results should be applied to the same area. It is worthwhile noting that, in this way, more than eight thousand Italian municipalities could be geologically classified based on realistic data, and *AF* values could be consequently attributed.

In order to apply the results presented here to the Italian territory, and possibly integrate them to the seismic hazard maps, Fig. 1 and Table 1 were composed into a form. This last was sent by the Dipartimento della Protezione Civile - Servizio Sismico Nazionale to the technicians of small towns and villages of a first group of six Regions of central-southern Italy (Marche, Abruzzo, Molise, Latium, Sicily, and Calabria) and is going to be sent to the rest of the Italian municipalities.

Technicians were asked to classify their small towns or villages by filling in the form. At the moment, we are collecting these returned forms and organising the data into a database and a GIS, therefore making the association of the results of the numerical modelling here presented to every Italian small municipality possible. In this way, the *AF* values could contribute to define a first estimate of the role played by the local geology to bedrock-referred SHA at a large scale.

Table 1 - S wave velocity classes adopted in this work for the main lithotypes.

Velocity class	Lithotypes (rocks and soils)	S wave velocity (*Vs*)
A1	Crystalline rocks (gneiss, granite, etc.), carbonate rocks (dolostones, limestones, marly limestones), ancient cemented carbonate breccias, evaporites, …	>1500 m/s
A2	Marls, sandstones, flysch deposits, conglomerates, Quaternary cemented talus, shales, overconsolidated clays, multicoloured clays, welded tuffs, fractured carbonate rocks, …	800-1500 m/s
B	Clayey marls, clays, badly cemented sandstones, sands, weathered tuffs, gravels, loose debris, …	400-800 m/s
C	Sandy-gravel alluvial deposits; silty-sandy alluvial deposits, "terre rosse", …	200-400 m/s
D	Loose silty clays, talus, stable landslides, silts, sands, lacustrine clays and sands, …	100-200 m/s
E	Organic clays, peats, anthropic covers, active landslides, liquefiable soils, …	<100 m/s

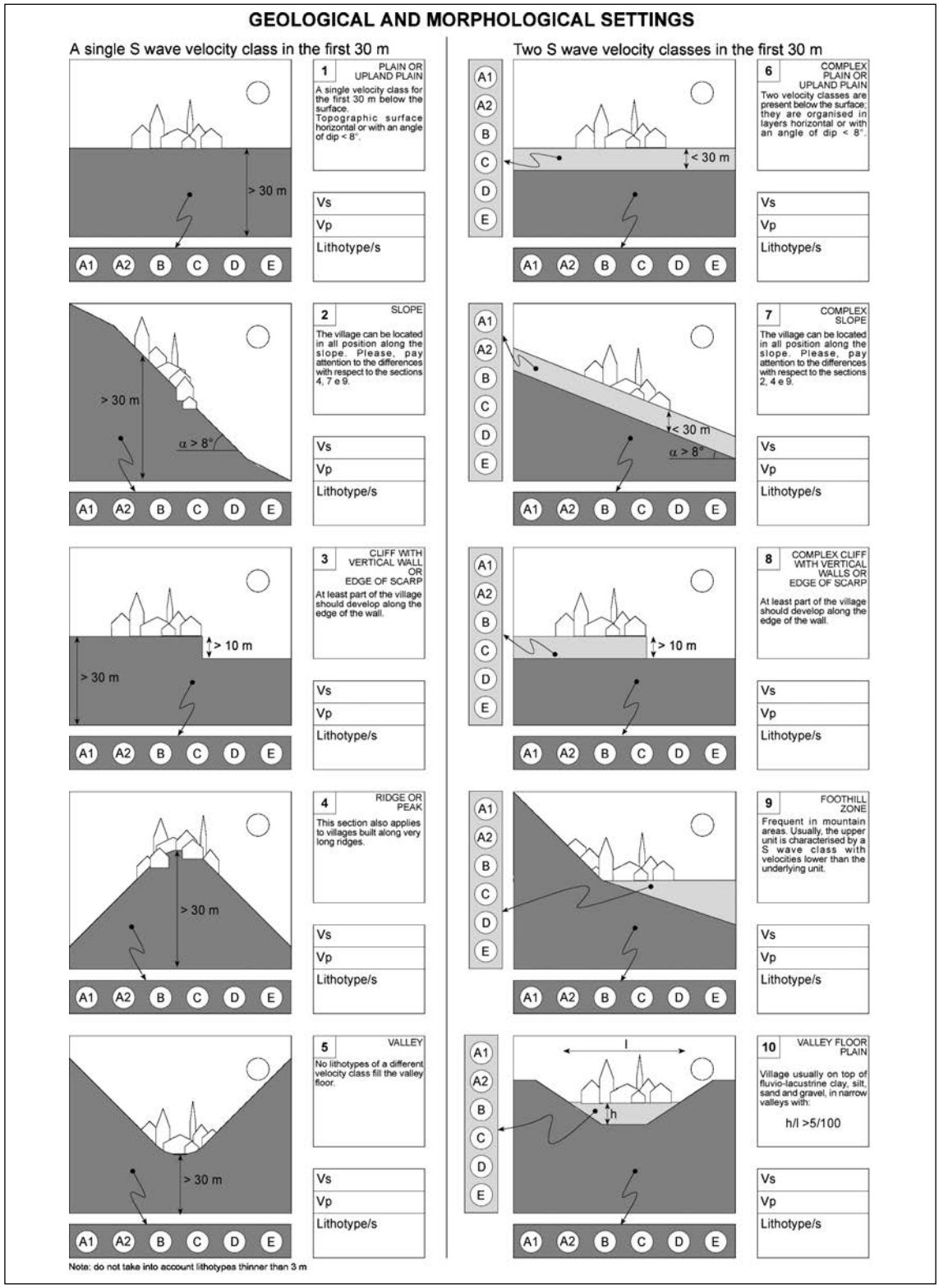

Fig. 1 - Grid of schematic cross-sections based on the most common geological and morphological settings present in the Italian territory.

2. Definition of the geological settings

The first step for the definition of the geological setting of each small town or village was the design of a table of lithotypes grouped into six S-wave velocity (*Vs*) classes (Table 1), and of a grid of ten schematic geological cross-sections representing, for the first tens of metres, the most common geological and morphological settings occurring in the Italian territory (Fig. 1).

The *Vs* classes (Table 1) were chosen according to some commonly accepted classifications available in literature (Pergalani *et al.*, 1999, 2000; Ferrini *et al.*, 2000, Wills *et al.*, 2000) and, in particular, to the European codes (Eurocode 8, 2001).

The cross-sections of Fig. 1 schematise the shallowest part of the geological and morphological settings. The first five sketches (schemes 1-5, left column of Fig. 1) are related to different morphologies but homogeneous rock properties (i.e. they can be characterised by a single *Vs* value class and a gradient). The last five sketches (schemes 6-10, right column of Fig. 1) involve a contrast of impedance between rocks that can be described by two Vs value classes and their relative gradients. In these cases, we assume that ground motion is affected both by the acoustic impedance contrast between the geological units, and morphological effects.

In detail, cross-sections 1 and 6 represent cases with no morphological contribution. Cross-sections 2-7 and 3-8 represent sites located along slopes or at the edge of morphological scarps, such as cliffs or fluvial terraces, respectively. Cross-sections 4 and 5 identify morphologies typical of ridges and valleys; sections 9 and 10 represent foothills and flat floor valleys that can be usually observed in Italian mountain regions.

Taking into account all the combinations of lithotypes and morphological features, a total of 180 models are theoretically possible, but some of them cannot be considered realistic. For instance, in our modelling we did not consider cases with very low velocity materials underlying high velocity ones (A overlying E in sketches 6-10), and we reduced the number of performed analysis to 157 models.

According to the literature (Wills *et al.*, 2000, and references therein), we referred to a thickness of a few tens of metres when describing the geological settings. Given the velocity ranges for different lithotypes, impedance contrasts at higher depths induce amplifications at low frequencies (< 2 Hz) that are not significant for the majority of buildings present in the Italian small towns and villages (masonry and low R.C. buildings). The geometries and lithologies considered in this study are very simplified and obviously do not represent all the possible cases.

3. Physical parameters of the geological settings

The Italian strong motion data used in seismic hazard analysis (and which the attenuation laws are based on) are recorded at rigid sites characterised by surface *Vs* velocity of about 800-1000 m/s; therefore, the methodology applied here refers to a site located at the surface and characterised by the same velocities. As a consequence, in the numerical modelling we decided to use a bedrock velocity value of 800 m/s (class A in Table 1), both in the homogeneous models (Fig. 1, left column) and in the halfspace for the two-layer models (Fig. 1, right column). However, many of these models are not formed by class A lithotypes (Table 1), and a 800 m/s bedrock is not always present in the schemes of Fig. 1. Needing such a bedrock, we decided to introduce this, where necessary, by applying a velocity gradient from a depth of 30 m to increase the velocity with depth up to the value of 800 m/s.

For all layers with a thickness grater than 30 m and for the halfspace, the velocity gradient is derived from the range of each class according to the following relationship:

$$gradV = \frac{V_2 - V_1}{30}$$

where V_2 is the maximum and V_1 the minimum velocity of shear waves in each class (e.g.: for class C, V_2 = 400 m/s, V_1 = 200 m/s; see Table 1 and Figs. 2 and 3). This gradient is kept constant up to a velocity equal to that of the reference site (800 m/s). In the geological schemes of Figs. 2 and 3, H is thickness where the velocity increases with depth as far as the value of 800 m/s. As the dip of the gradient depends on the velocity class (i.e. on V_1 and V_2), H is not constant.

We used this velocity distribution in all the homogeneous cases (Fig. 1, left column) and for the deepest layer in the other cases (Fig. 1, right column).

In order to apply the results of this work to large scale SHA, further assumptions were needed in the modelling of the geological schemes of Fig. 1. These assumptions are described in the following.

Schemes 2 and 7 were considered equivalent to 1 (Fig. 2a) and 6 (Fig. 3a) respectively, but with a different incidence angle of the incoming waves. Concerning scheme 3 (Figs. 1 and 2b), we decided to assume a cliff 15 m high in case of soft soils (C, D and E in Table 1) since higher values are not realistic for low velocity deposits, and 30 m high in case of other lithotypes. This choice represents an attempt to model amplification effects in the frequency range of interest for buildings (>1 Hz). Figs. 2c and 2d show details of schemes 4 and 5 of Fig. 1, that represent a ridge and a valley. For the ridge analysis we had to define its geometry (slopes' dip, relief height, and the width of the flat area at its top). We assumed a trapezoidal geometry with the following dimensions: slopes' dip = 30°, relief height = 50 m for soft soils (C, D and E in Table 1) and 200 m for the rigid ones, upper base = 100 m. For the valley analysis (Fig. 2d) we used the same values referring to a geometric scheme horizontally specular to that of the ridge.

The shallowest layer of schemes 8 to 10 of Fig. 1 is assumed to be homogeneous with a constant shear velocity *Vs*.

The scheme of Fig. 3b is similar to that of Fig. 2b, except for the cliff lithotype, that is different from the underlying lithotype. This last can be either more or less rigid with respect to the upper one.

Fig. 3c (scheme 9 of Fig. 1) represents part of a large valley bounded by a relief; the modelled site is located at the extreme end of the valley, just along the relief foothills. We decided to assign an angle of 30° to the relief slope, an angle of 10° to the buried slope and a maximum thickness of 30 m for the deposit that fills the valley. The width of the site, where the response spectra were computed, is 170 m wide, and corresponds to the length of the transition zone where the bedrock underlying the valley fill slants.

Finally, for the scheme of Fig. 3d (scheme 10 of Fig. 1), which represents a narrow valley between two reliefs, we considered an unique slope dip of 30° both for relief and buried bedrock. We also assumed a 30 m deep valley and, accordingly, a 600 m wide one.

In order to quantitatively characterise the schemes of Fig. 1 for the analyses, we assigned mean values to the parameters describing the modelled lithotypes. As said in the Introduction, we excluded all the known and extreme cases of amplification values, because these are out of the

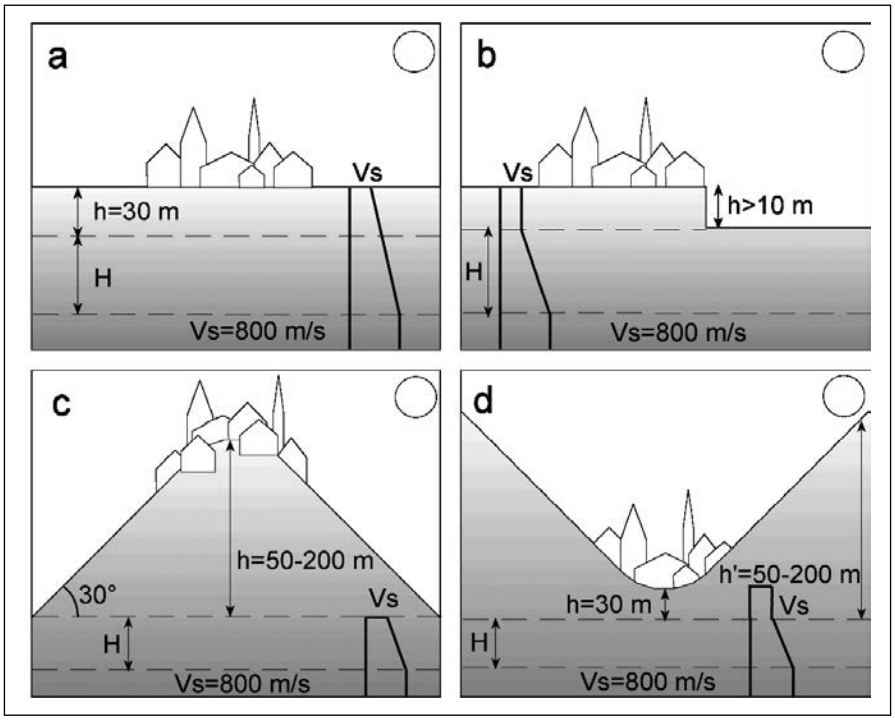

Fig. 2 - Configuration of the cross-sections used for numerical modelling: a) scheme 1 from Fig. 1; b) scheme 3 from Fig. 1; c) scheme 4 from Fig. 1; d) scheme 5 from Fig. 1.

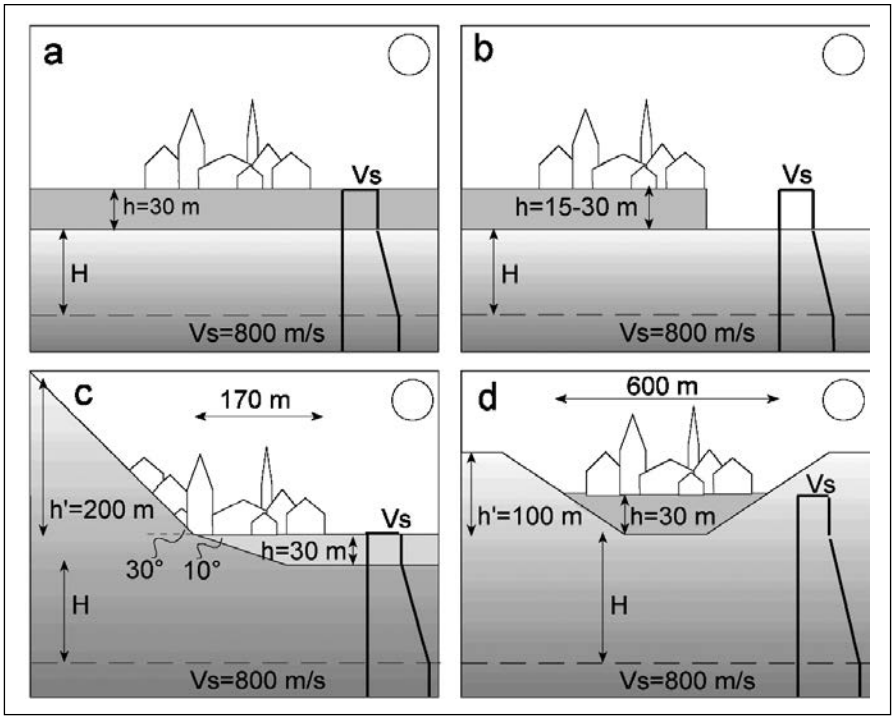

Fig. 3 - Configuration of the cross-sections used for the numerical modelling: a) scheme 6 from Fig. 1; b) scheme 8 from Fig. 1; c) scheme 9 from Fig. 1; d) scheme 10 from Fig. 1.

scope of this work and should be considered only in microzoning analyses.

Regarding the mechanical properties of lithotypes, and particularly their dependency on the level of shear deformation, we made very simple approximations. We acquired the shear modulus and damping relationships from Italian literature (microzonation of Umbria and Marche Regions, Central Italy: Pergalani *et al.*, 1999, 2000), particularly those referring to materials described as sand, clay, silty-clayey fluvial-alluvial deposits, and sandy-gravel fluvial-alluvial deposits. We do not consider the relationships for very low quality deposits. In Figs. 4a and 4b the degradation curves, respectively for G/G_0 and damping, are shown as function of the shear deformation γ%.

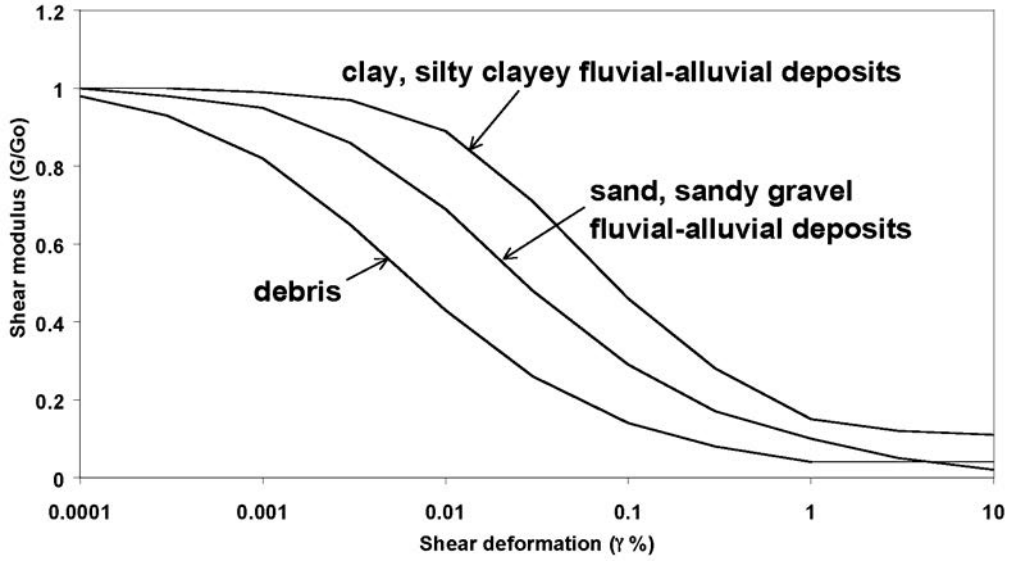

a)

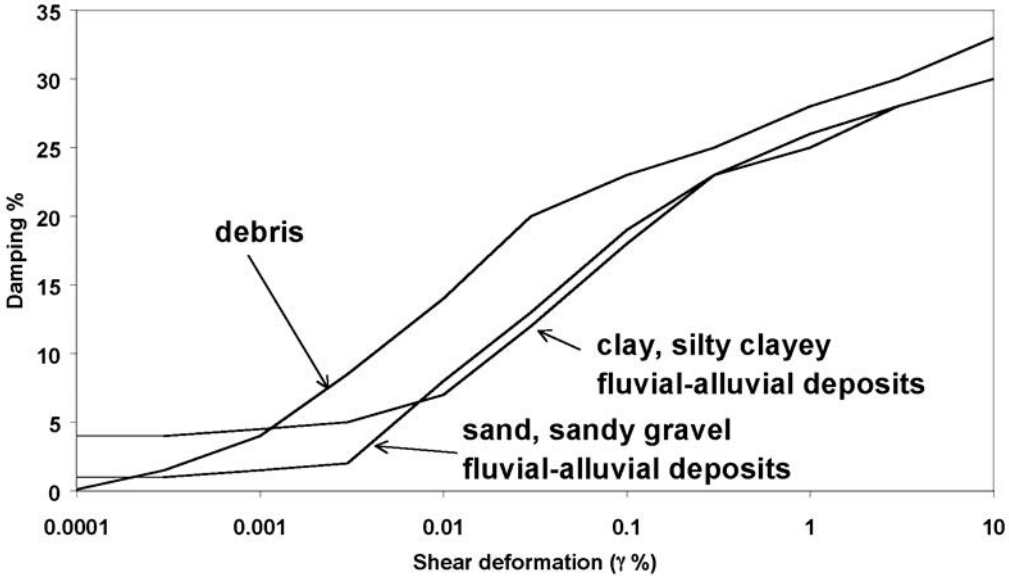

b)

Fig. 4 - Degradation curves: a) shear modulus vs. shear deformation; b) damping vs. shear deformation.

In Fig. 4a, G_0 is the shear modulus at very low deformation, and $\gamma = 0.0001\%$. These curves are a good representation of the mean value of the degradation laws for these lithotypes. This was confirmed by the analysis of some typical and known rocks in different Italian regions, and by a comparison of the obtained results with literature data (Seed and Idriss, 1970; Seed *et al.*, 1986; Sun *et al.*, 1988; Pergalani *et al.*, 1999, 2000).

4. Numerical modelling

4.1. Seismic input

For each model, we used three synthetic input motions in order to obtain the expected ground motion for three energy levels (PGA = 0.13 g, 0.20 g, and 0.27 g). The use of different levels of excitation takes into account the modification of the mechanical properties of rocks with their shear deformation. These input motions derive from mean values of the hazard spectra calculated on the basis of the hazard studies for the Italian territory (Albarello *et al.*, 2000). Such mean values are shown in Fig. 5.

A further assumption is that the reference input motion was generated by plane shear waves (S waves) vertically impinging on the surface. This is valid if the seismic source is very far and the incoming time history is only made by S waves. Schnabel *et al.* (1972) showed that such an assumption is still valid also in case of inclined and other types of waves.

As already mentioned, the site amplification was evaluated computing the spectral ratio with respect to a reference site. The latter is defined as a rock, outcropping with a flat horizontal surface, characterised by a stiffness equal to the minimum value of type A rock, that is, a *Vs* of 800 m/s. We considered 14 period values of the spectral ratios, the same used for the hazard analysis of the Italian territory (Albarello *et al.*, 2000; Table 2).

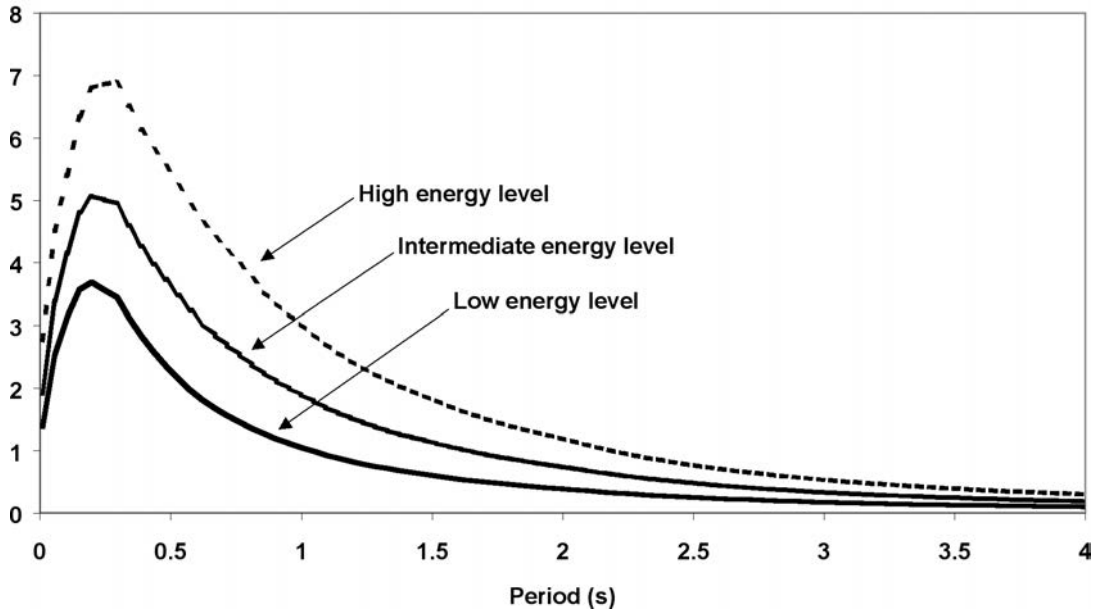

Fig. 5 - Spectra of the reference seismic inputs.

4.2. Computer codes

The geological schemes 1 and 6 of Fig. 1 are different from the others, as they refer to a horizontally layered configuration. In case of vertically incoming plane waves, they can be modelled with a 1D scheme, while the other cases need a 2D scheme. Therefore, we used two different computer codes: PSHAKE (1D; Sanò and Pugliese, 1991; Sanò *et al.*, 1993) and BESOIL (2D; Sanò, 1996; Pergalani *et al.*, 2002).

PSHAKE is based on the same algorithm as SHAKE (Schnabel *et al.*, 1972; Fig. 6a) but allows directly using a response spectrum instead of a time history as input (Romo-Organista *et*

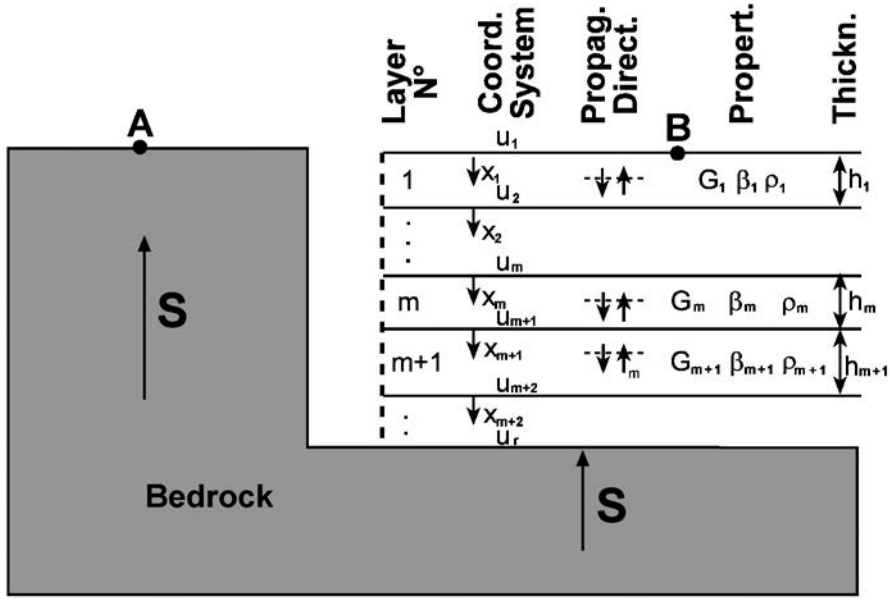

Fig. 6 – a) Scheme 1D from PSHAKE (Sanò *et al.*, 1991). b) Scheme 2D from BESOIL (Sanò, 1996). Rock parameters: G = shear modulus; β = damping; ρ = density; μ, λ = Lamè constants.

al., 1977). A power spectrum of a family of ground motions on the outcropping rock is obtained through an iteration on the given acceleration response spectrum, taking into account its exceedance probability.

The computer code BESOIL (Sanò, 1996; Fig. 6b) is based on the Boundary Element Method (BEM; Brebbia, 1984), applied to wave propagation in rocks. This method provides advantages over domain approaches, i.e. the Finite Element Method (FEM), due to the reduction by one of the problem dimensions, the relatively easy fulfilment of radiation conditions at infinity, and the high accuracy of results. The method is based on the mathematical work on integral equations as formulations of linear boundary value problems as an alternative to those in terms of partial differential equations. BESOIL (Sanò, 1996) uses the indirect method and follows the works of Sanchez-Sesma and Campillo (1991) and of Sanchez-Sesma *et al.* (1993) strictly.

Let us consider the space in Fig. 6b, in the homogeneous infinite domain below the valley to the right of the relief, under the incidence of elastic waves. The resulting motion is given by the free-field motion (i.e. the incident waves) and the 'scattered' motions (i.e. the waves reflected, diffracted and refracted from the valley boundary). In fact, in this irregular configuration, the ground motion comes, in physical terms, from the interference of incoming waves with those generated by the boundary. On the other hand, in limited areas of the valley, e.g. to the extreme right-hand side of Fig. 6b (far from the valley boundary), the motion is only due to diffracted waves. They are numerically generated by point sources distributed on the same layer interfaces where they are physically created. Imposing the continuity conditions over the boundary between adjacent homogeneous regions and the conditions of null stress on the interface with the air, the integral equations can be transformed into a system of algebraic equations and solved in the unknown point source. As in PSHAKE (Sanò *et al.*, 1991), the analysis is made in the frequency domain and it is possible to use the PSHAKE (Sanò *et al.*, 1991) response spectrum directly as input. Since the code can only perform linear analyses, the non-linearity is taken into account using an equivalent linear analysis as in SHAKE (Schnabel *et al.*, 1972) and PSHAKE (Sanò *et al.*, 1991) cases.

4.3. Seismic output

Along the geological sections, the output spectra were computed for 7 to 12 points (depending on the scheme in question), equally spaced on a length of 100 m along the surface.

The mean value of the computed spectra was assumed to be representative for every analysed scheme. Such an assumption can be accepted because, as seen before, only small municipalities are considered; sites spread over large areas and characterised by different geological and morphological settings are, on the contrary excluded.

In the end, this methodology gives two kinds of seismic output: (i) the mean response spectra for the three energy levels of seismic input and for the different geological settings, and (ii) the related *AFs*.

The *AF* is defined as follows.

A Spectral Intensity (*SI*; Housner, 1952) was computed in a period range of 0.1-0.5 s:

$$SI(PSV) = \int_{0.1}^{0.5} PSV(T, 0.05)dT$$

where *PSV* is given by the pseudo-velocity spectral ordinates, *T* is the period, and 0.05 is the damping. The spectral intensities were computed for the following seismic motions:

SI_{input}, mean spectral intensity for the reference spectrum;

SI_{output}, mean spectral intensity for the each computed amplification spectrum.

AF was defined on the basis of the following ratio:

$$AF = \frac{SI_{output}}{SI_{input}} \ .$$

It represents the mean value of the velocity spectrum ratio in the high frequency range. Therefore, it only gives a general indication of the motion amplification for the low period range, referring to low masonry constructions or stiff buildings, but not to more flexible structures like isolated ones.

5. Results and interpretation

In Fig. 7a, the spectral ratios for scheme 1 of Fig. 1 are shown as function of the period. They are the ratios of the mean computed spectra with respect to the reference one, for the 14 periods quoted in Table 2. Each mean spectrum is computed for 7 points equally spaced on the surface where the centre of the site is located. The lithotypes (A-E of Table 1) are labelled on each group of three curves, which correspond to the three different input motions (1-3, from the highest to the lowest energy levels). For the lithotype A, whatever the seismic input energy level, $AF = 1.0$ by definition.

Table 2 - Period values where amplification spectral ratios are computed (in seconds).

T1	T2	T3	T4	T5	T6	T7	T8	T9	T10	T11	T12	T13	T14
0.04	0.067	0.1	0.15	0.2	0.3	0.4	0.5	0.75	1.0	1.5	2.0	3.0	4.0

At low periods, the maximum amplification always occurs for low input motion (curves labelled with 3). Notice that the variation of the effect due to the input intensity is greater for softer rocks while it is almost null for lithotype B. This is due to the shear deformation (and consequently to the stiffness degradation and energy dissipation) that, under the same vibratory load, is less for stiffer rocks than for softer ones. The peak values of each curve move toward greater periods as the rock stiffness decreases. The lithotype E is peculiar, because it is defined as very soft soil ($Vs \leq 100$ m/s) and, under the seismic shaking, it degrades to much lower stiffnesses. Therefore, for this kind of soil, the problem is not the amplification of the motion but its bearing capacity. We decided, consequently, not to consider it in the following analyses. We suggest, instead, to carry out specific analyses on this class of lithotypes in developing hazard studies. In Fig. 7b the related *AFs* are shown.

Scheme 2 of Fig. 1 is considered as equivalent to scheme 1 of the same figure, because the only difference is given by the incident angle of impinging waves. Therefore, we decided to assign the same results obtained for scheme 1 to this geological setting.

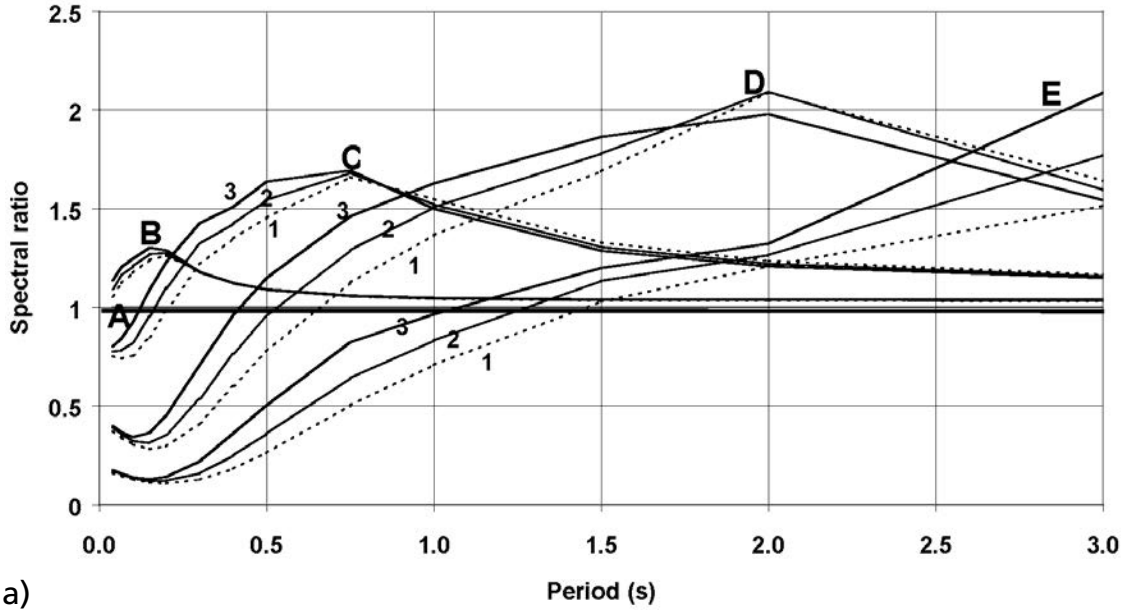

a)

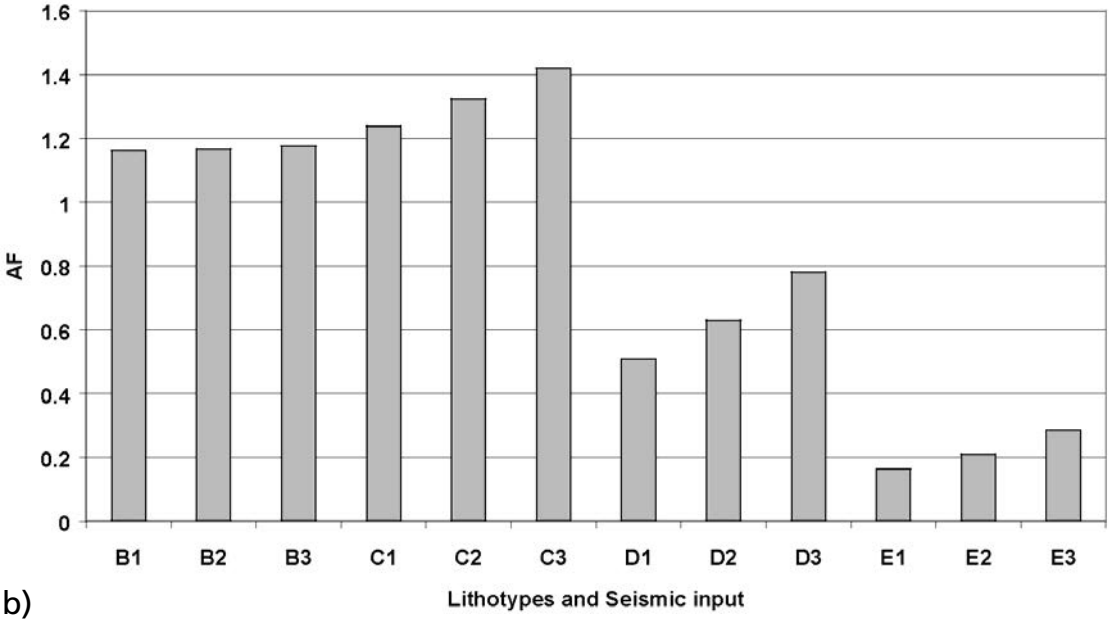

b)

Fig. 7 - Spectral ratio (a) and *AF* (b) from the analysis of scheme 1. For lithotype A, whatever the seismic input energy level, *AF* = 1.0 by definition.

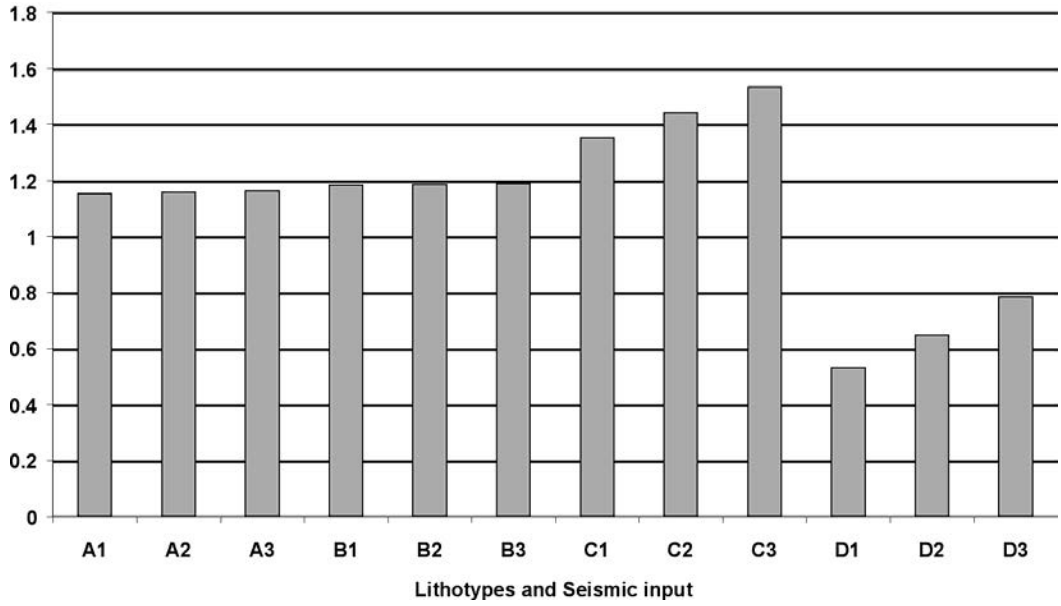

Fig. 8 - *AF* for scheme 3.

Fig. 8 shows the *AF* for the cliff (scheme 3 of Fig. 1). With respect to scheme 1 of Fig. 1, the presence of the cliff induces an *AF* increase of about 15% for the lithotype A and of about 10% for the lithotype C. For lithotypes B and D, *AF* values remain nearly equal. Notice that the lithotype D induces a deamplification whatever the morphology, flat or with a cliff.

Fig. 9a shows the spectral ratios for the ridge (scheme 4 of Fig. 1). Comparing this with Fig. 7a, two effects can be observed that influence the shape of the curves. The first is the effect of the rock stiffness (the same described for scheme 1), and the second is the oscillation of the ridge, that behaves as a shear deformable structure, with a natural period proportional to *Vs/H*. The first effect dominates in case of soft soils, and the second in case of rigid rocks. In detail, concerning lithotype B, the amplification at low periods (about 0.2 s) is similar to that of scheme 1 and it is due to the first effect, while the plateau in the range of greater periods is due to the second effect. Similarly, in the case of the valley (scheme 5 of Fig. 1; Fig. 9b), there is a general reduction of the motion due to the topographic effect, in contrast to the soft soil effect that dominates in the case of lithotypes C and D. For lithotype B, the *AF* is 1.25 and represents the mean value of the spectral ratio in the period range of 0.1-0.5 s. It is worthwhile noting that the same factor, when computed in the range of 0.5-2.0 s (thus concerning long period structures) is 1.5.

The results for horizontally layered setting with a stiffness contrast between two different lithotypes (scheme 6 of Fig. 1) are shown in Figs. 10a and 10b. For the sake of simplicity, only the curves related to the high energy seismic input are shown. For increasing impedance contrasts, the peak values of amplification increase and move toward longer periods. As the amplification is computed for a reference site characterised by $Vs = 800$ m/s, cases encompassing lithotypes different from A provide amplification values that derive from the sum of two

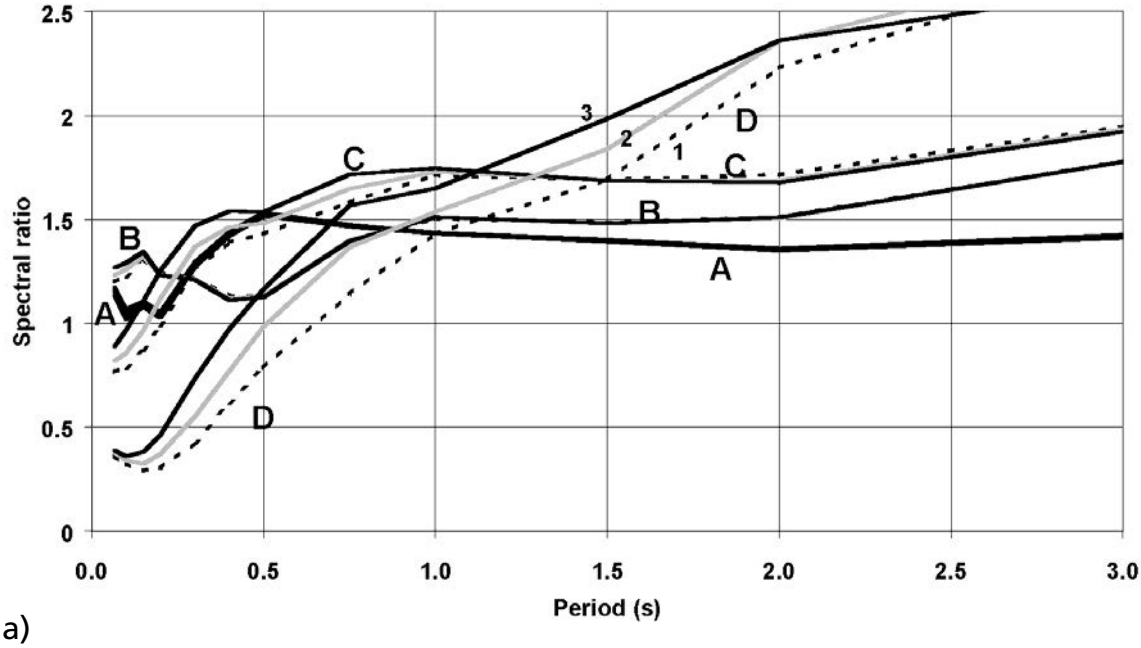

a)

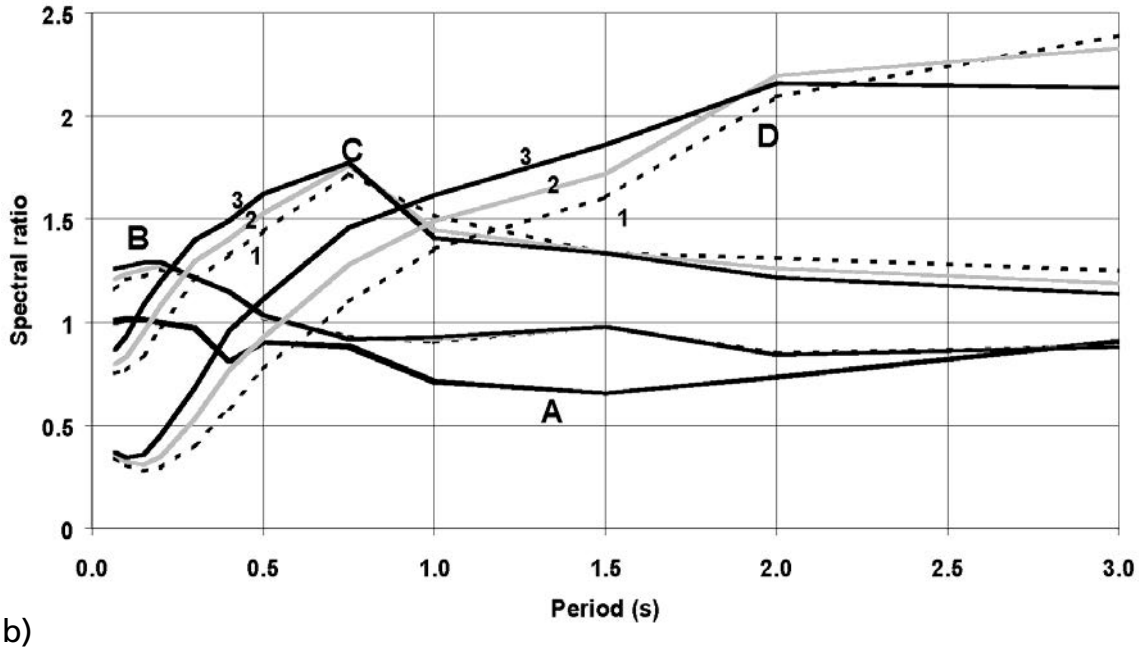

b)

Fig. 9 - Spectral ratio from the analysis of scheme 4 (a), and from scheme 5 (b).

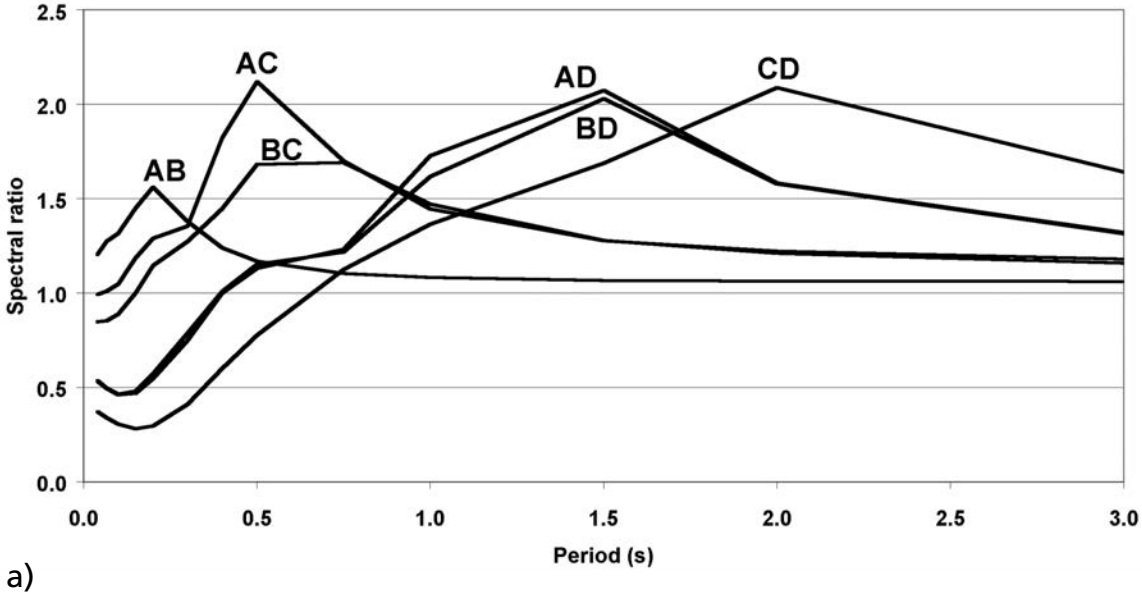

a)

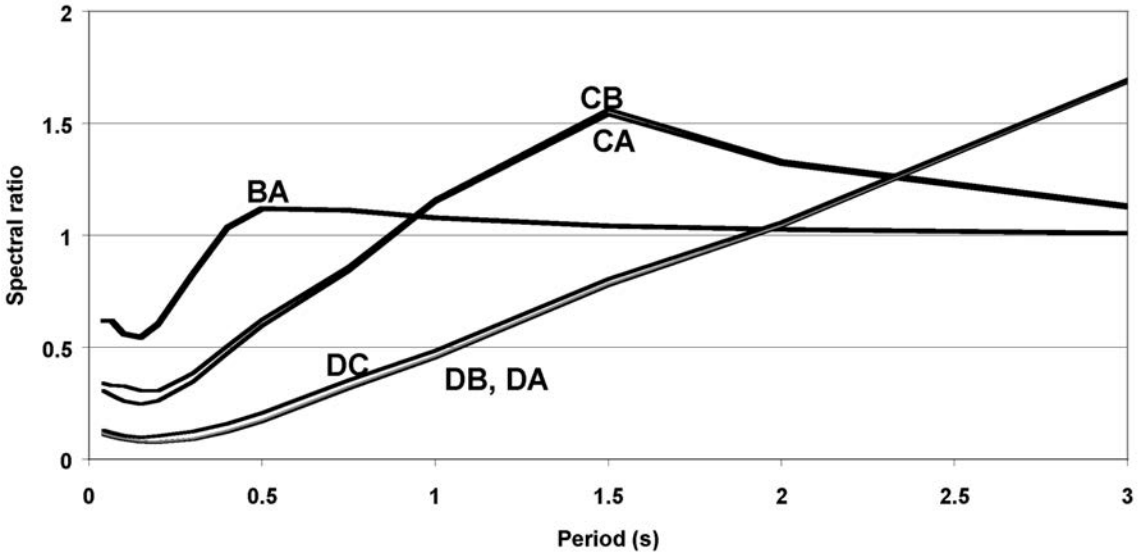

b)

Fig. 10 - Spectral ratio for high energy level from the analysis of Scheme 6 in the case of soft soil on rigid rock (a), and in the case of stiff rock on soft soil (b). The two letters that label the curves identify the two layers (Fig. 6a); the first refers to the lower.

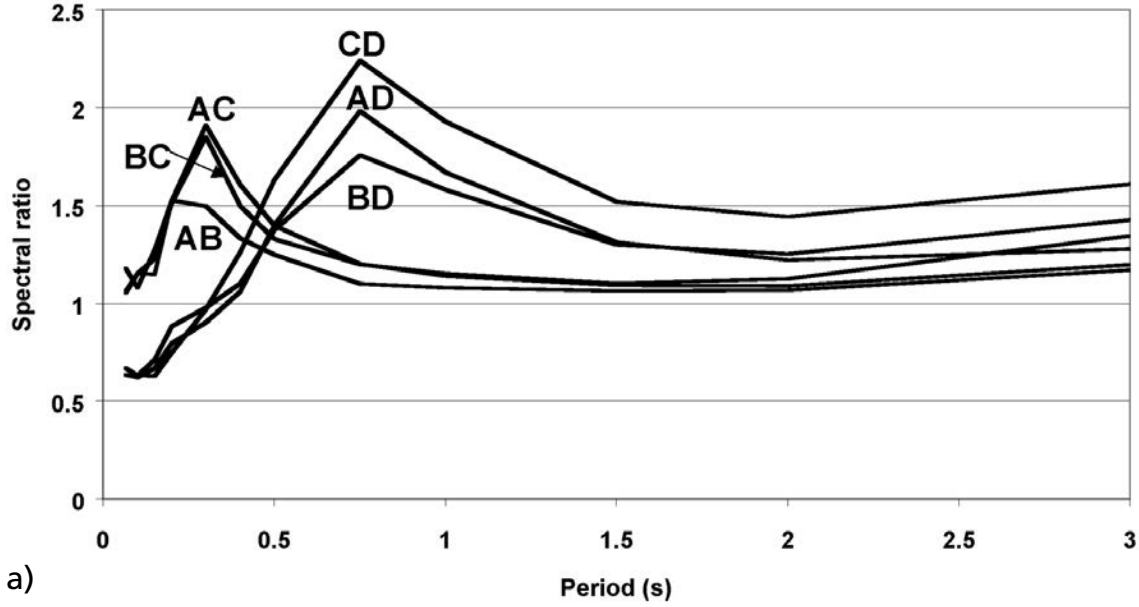

a)

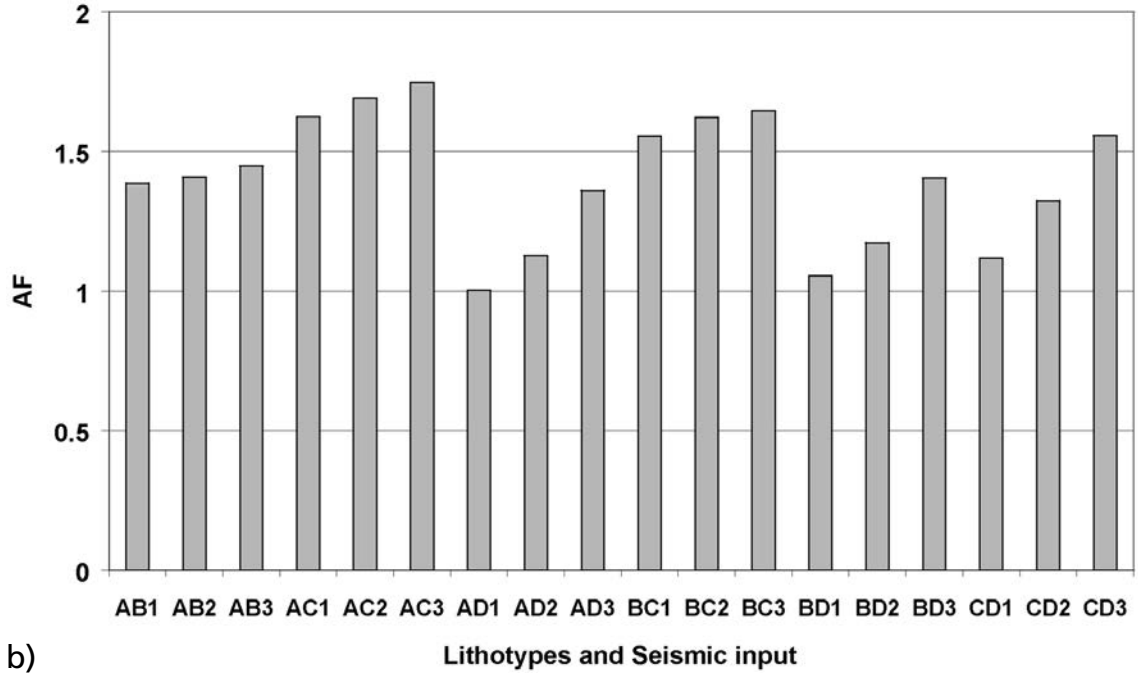

b)

Fig. 11 – Spectral ratio for high energy level from the analysis of scheme 8 (a), and *AF* for the three energy levels referring to scheme 8 (b).

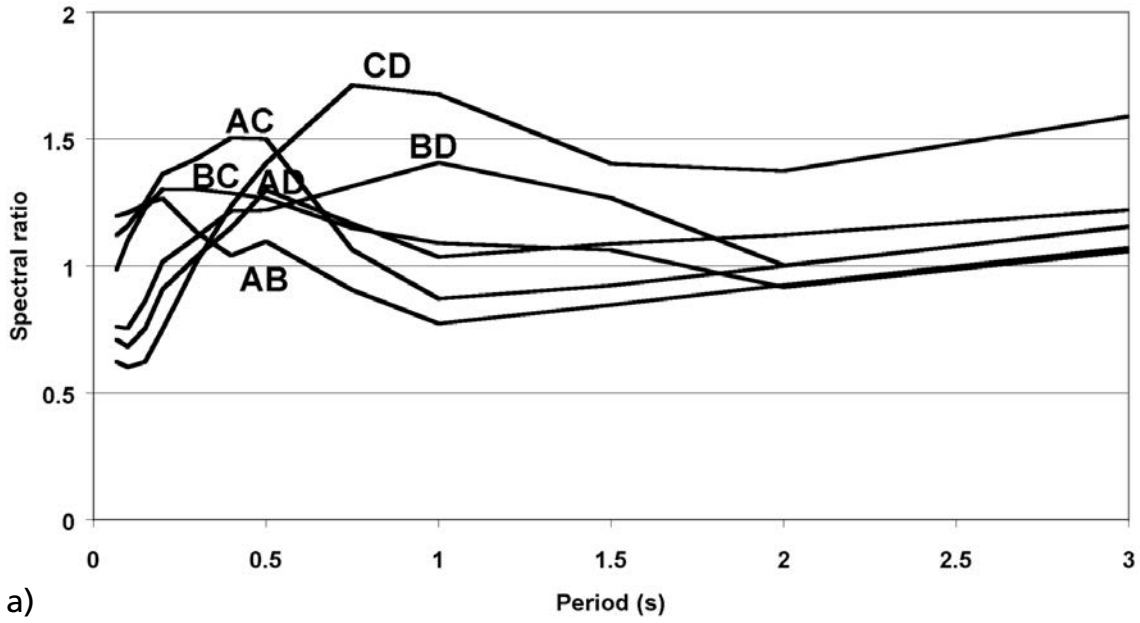

a)

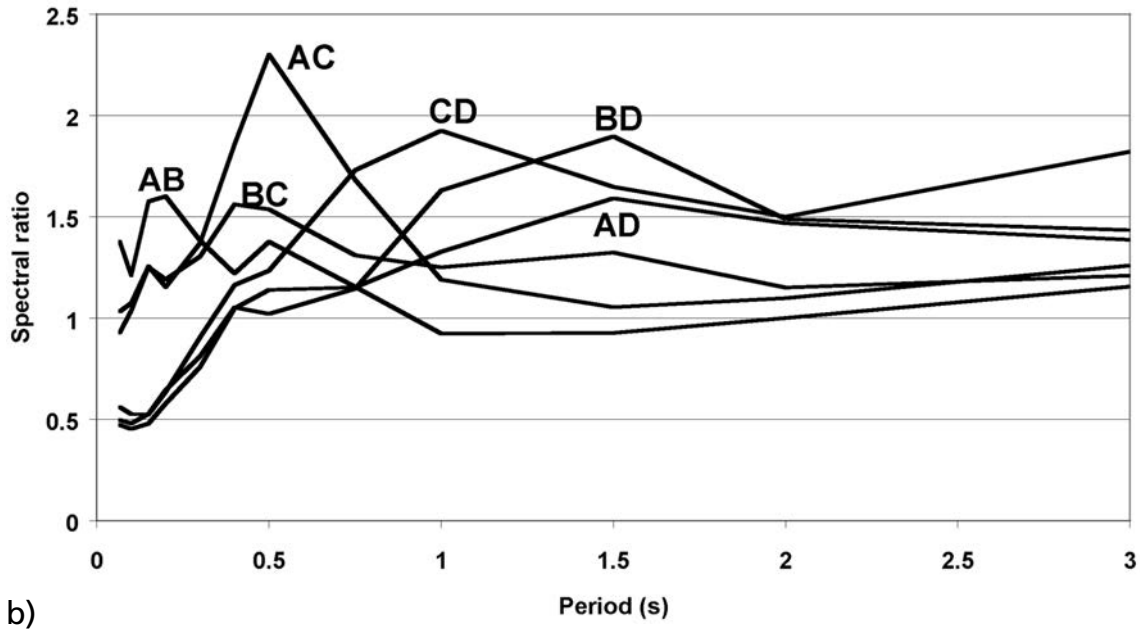

b)

Fig. 12 – Spectral ratio for high energy level from the analysis of scheme 9 (a), and from the analysis of scheme 10 (b).

contrasts: between the upper and lower lithotypes, and between the lower lithotype and the underlying halfspace.

The upper lithotype can be either softer (Fig. 10a), or stiffer than the lower one (Fig. 10b). In the first case, amplification effects can be observed. In the second case, a general deamplification occurs for short periods (T < 1 s) and this is quite evident if the lower lithotype is particularly soft (e.g., D).

Scheme 7 of Fig. 1 is considered equivalent to scheme 6 of the same figure, because also in this case the only difference is given by the incident angle of impinging waves.

In the case of a complex cliff (scheme 8 of Fig. 1), the results in case of rigid lithotypes (A-C) underlying the cliff lithotype (Fig. 11a) are not too different from those for the complex plain of scheme 6 (Fig. 1). A difference arises in the case of a cliff formed by lithotype D: the pick values move toward lower periods, i.e. toward the frequency range typical of civil constructions. This is confirmed by the *AF* shown in Fig. 11b, which are greater than 1.0 also for soft soils.

Results for a large valley at the foothills of a relief (scheme 9 of Fig. 1) and for a narrow valley floor plain between two reliefs (scheme 10 of Fig. 1) are shown in Figs. 12a and 12b, respectively.

It is not surprising that, considering both figures, the amplification of a two-layered scheme made up of classes A and D (curve AD in Fig. 12a), is lower than that made up of classes C and D (curve CD in Fig. 12a), even if the first case shows a greater impedance contrast. As a matter of fact, these results are due to both the impedance contrast between the upper lithotype and the lower one, and the amplification between the lower lithotype and the underlying halfspace.

Comparing schemes 6 and 9 of Fig. 1 and the related diagrams (Figs. 10a and 12a, respectively), we observe that for the foothill zone a high impedance contrast moves the maximum amplification toward higher frequencies. These frequencies can be particularly dangerous for low-rise buildings. Amplification effects due to surface waves generated at the valley boundaries are, however, not noticeable when compared to those due to the impedance contrast. This probably depends on the vertical incidence of the incoming waves, and on the specific geometry considered, particularly the slope of the edges, and the depth and the width of the valley. Larger slopes and higher depths of the valley could probably generate surface waves and focalisation effects. In the case shown, such focalisation effects are reduced because the average of the output spectra was calculated on a width of about 170 m.

6. Comparison with real cases

In order to evaluate the reliability of the results obtained, we compared them with the *AF* values for real cases analysed with different degrees of detail.

As the numerical modelling and the computer codes used are usually applied and widely accepted in the international literature, their discussion is considered beyond the aim of this paper.

As seen before, the table of lithotypes, grouped in six S-wave velocity classes (Table 1), is derived from some commonly accepted classifications available in literature (Pergalani *et al.*, 1999, 2000; Ferrini *et al.*, 2000; Wills *et al.*, 2000) and from the European codes (Eurocode 8, 2001). Although *Vs* values acquired *in situ* on the Italian territory are rare, those available fall perfectly within the proposed classes [for instance, see the seismic characterisation of the

shallowest soils of the town of Fabriano described by Marcellini and Tiberi (2000), and the study along the High Tiber Valley by Crespellani *et al.* (2002)].

Concerning the geological cross-sections modelled, all the classifications adopted in the main Italian microzonation studies carried out in the last decades (Table 3 and references therein) can be recognised in the geological schemes of Fig. 1, which in general show a higher degree of detail.

With regard to the seismic input, the chosen mean values of hazard spectra correspond to those used by Albarello *et al.* (2000) in the hazard maps of Italy.

Table 3 - Comparison between the geological schemes adopted in this work (Fig. 1) and other geological and morphological classifications available in Italian literature. Classes E1, E2, E3 in Pergalani *et al.* (2000) and zones of rockfall, landslide, liquefaction, or differential compaction in CNR-PFG (1983) correspond to coseismic phenomena, and therefore have not been considered.

Geological schemes of Fig. 1 in this work	**CNR-PFG (1983)**	**CNR-Regione Lombardia (1996)**	**Pergalani *et al.* (2000)**	**Crespellani *et al.* (2002)**
1 – Plain or upland plain			E4	
2 - Slope	Pendii (slopes)	Pendii (slopes)	E4	Pendio (slope)
3 – Cliff with vertical wall or edge of scarp	Terrazzi (terraces)	Scarpate (scarps)	E5	Scarpata (scarp)
4 – Ridge or peak	Creste rocciose sottili (sharp rocky ridges)	Dorsali (ridges)	E6	Cresta (ridge)
5 – Valley		Valli (valleys)	Valle (valley)	
6 – Complex plain or upland plain			E4, E9	
7 – Complex slope	Pendii (slopes)	Pendii (slopes)	E4	Pendio (slope)
8 – Complex cliff with vertical wall or edge of scarp	Terrazzi (terraces)	Scarpate (scarps)	E5	Scarpata (scarp)
9 – Foothill zone		Conoidi (fan deltas)	E8	
10 – Valley floor plain		Valli (valleys)	E7, E9	Valle (valley)

Finally, a comparison between the mean *AF* values obtained for the proposed schemes (Fig. 1) and those obtained for real geological cases can be attempted, although we remind the reader that we are not dealing with a microzonation. For instance, let us consider the study of Cesi village, carried out by Pergalani *et al.* (1999) after the 1997-98 Umbria-Marche earthquake. The geological setting of this village is given by an alluvial plain bordered by a carbonate slope. This setting is particularly important because it is one of the most complex in Fig. 1, but it is also an extremely frequent geological condition in Italy.

For such a study, Pergalani *et al.* (1999) collected geological, geomorphological, geotechnical and geophysical information in order to realise a refined geological cross-section from the plain to the slope. This section was analysed with the aid of dynamic codes to calculate the possible local effects under an input motion. In this way, *AF* values were available in different points along the section. The *AF* values obtained range from 0.8 to 1.6, with an average value of 1.3.

The real case described clearly fits into scheme 9 of Fig. 1. In particular, the rocks modelled there correspond to lithotypes A (slope) and C (alluvial plain) on Table 1. Moreover, the

seismic input used by Pergalani *et al.* (1999) is comparable with our intermediate energy level seismic input. The *AF* value obtained in the present work from the modelling for such a configuration is 1.3.

This case constitutes an example of validation of the results of the present study and it allows us to better explain the meaning of the *AF* values obtained. As a matter of fact, each *AF* value obtained synthesises a complex geological setting, which in reality would be characterised by many different *AFs*. However, the comparison with real cases shows that each *AF* value we obtained is an expression of the mean behaviour of the site, and therefore can be accepted for the aims of this study (i.e., to define a first estimate of the geological contribution to the bedrock-referred SHA).

7. Conclusions

This study represents a first attempt to introduce an innovative simplified approach aimed at collecting information on the local geology of small towns and villages quickly, so as to define a first estimate of the geological contribution to the bedrock-referred SHA on a large scale.

This topic is quite important because, up to now, local geology has not been considered at a large scale, even if it can strongly modify the predicted ground motion at a site.

The methodology is developed for a large scale approach, therefore it cannot be used for building design purposes; however, once implemented, it could improve the quality level of seismic hazard maps available at a large scale.

Acknowledgments. Thanks are due to E. Priolo for his constructive criticisms and to A. Rovelli for his thoughtful review. We gratefully acknowledge D. Slejko for having strongly encouraged the publication of this work.

REFERENCES

Albarello D., Bosi V., Bramerini F., Lucantoni A., Naso G., Peruzza L., Rebez A., Sabetta F. and Slejko D.; 2000: *Carte di Pericolosità sismica del territorio nazionale*. Quaderni di Geofisica, **12**, 1-7.

Brebbia C.A.; 1984: *The boundary element method for engineers*. Pentech Press, London, 187 pp.

CNR-PFG; 1983: *Indagini di microzonazione sismica. Intervento urgente in 39 centri abitati della Campania e Basilicata colpiti dal terremoto del 23 novembre 1980*. CNR-PFG, Roma, Pubbl. **492**, 221 pp.

CNR-Regione Lombardia; 1996: *Determinazione del rischio sismico a fini urbanistici in Lombardia*. CNR, Milano, 148 pp.

Crespellani T., Madiai C. and Simoni G.; 2002: *Indagini geotecniche per la valutazione degli effetti di sito in alcuni centri dell'Alta Val Tiberina*. Ingegneria sismica, **19** (1), 15-32.

Eurocode 8; 2001: *Design of structures for earthquake resistance, PART 1: general rules, seismic actions and rules for buildings.* DOC CEN/TC250/SC8/N306, DRAFT n. 4.

Ferrini M. (Coord.), Foti S., Lo Presti D., Luzi L., Pergalani F., Petrini V., Pochini A., Puccinelli A., Signanini P. and Socco V.; 2000: *La riduzione del rischio sismico nella pianificazione del territorio: le indagini geologico tecniche e geofisiche per la valutazione degli effetti locali*. Relaz. interna, CISM, Lucca, unpublished.

Housner G.W.; 1952: *Spectrum intensities of strong motion earthquakes.* In: Proceedings of the Symposium on Earthquakes and Blast Effects on Structures, Earth. Eng. Res. Inst., Oakland CA U.S., pp. 20-36.

Marcellini A. and Tiberi P. (eds); 2000: *La microzonazione sismica di Fabriano*. CNR, GNDT, Regione Marche, 291 pp.

Pergalani F., Romeo R., Luzi L., Petrini V., Pugliese A. and Sanò T.; 1999: *Seismic microzoning of the area struck by Umbria-Marche (central Italy) Ms 5.9 earthquake of the 26 september 1997*. Soil Dynamic and Earthquake Engineering, **18**, 279-296.

Pergalani F., Petrini V., Romeo R., Pugliese A., Boscherini A., Checcucci R., Felicioni G., Luchetti L., Martini E., Motti A., Ponziani F., Simone G., Sorrentino A., Luzi L. and Sanò T.; 2000: *La microzonazione sismica speditiva relativa ai terremoti del 1997-98 in Umbria*. Regione dell'Umbria, CNR I.R.R.S., Milano, 233 pp.

Pergalani F., Petrini V., Pugliese A. and Sanò T.; 2002: *Seismic microzonation using numerical modelling*. In: Bull J.W. (ed), Numerical analysis and modeling in geomechanics, SPON PRESS, London.

Romeo R. and Pugliese A.; 1998: *A global earthquake hazard assessment of Italy*. In: Bisch Ph., Labbé P. and Pecker A. (eds), Proceedings of the 11th European Conference on Earthquake Engineering, A.A. Balkema, Rotterdam, pp. 115.

Romeo R., Paciello A. and Rinaldis D.; 2000: *Seismic hazard maps of Italy including site effects*. Soil Dynamics and Earthquake Engineering, **20**, 85-92.

Romo-Organista M.P., Jen-Hwa C., Lysmer J. and Seed H.B.; 1977: *PLUSH - A computer program for probabilistic finite element analysis of seismic soil-structure interaction*. UCB EERC report No 77/01.

Sanchez-Sesma F.J. and Campillo M.; 1991: *Diffraction of P, SV, and Rayleigh waves by topographic feature: a boundary integral formulation*. Bull. Seis. Soc. Am., **81**, 2234-2253.

Sanchez-Sesma F.J., Ramos-Martinez J. and Campillo M.; 1993*: An indirect boundary element method applied to simulate the seismic response of alluvial valleys for incident P, S and Rayleigh Waves*. Earthq. Engin. Struct. Dyn., **22**, 279-295.

Sanò T., Pugliese A. and Di Pasquale G.; 1993: *Aleatorietà del moto sismico nell'amplificazione locale*. In: Atti del 6° Convegno Nazionale "L'ingegneria Sismica in Italia", **1**, pp. 65-74.

Sanò T. and Pugliese A.; 1991: *PSHAKE - Analisi probabilistica della propagazione delle onde sismiche*. ENEA, Rapporto Tecnico RT/DISP/91.

Sanò T.; 1996: *BESOIL - Un programma per il calcolo della propagazione delle onde sismiche*. Italian National Seismic Survey, Rapporto Tecnico SSN/RT/96/9.

Schnabe1 P.B., Lysmer J. and Seed H.B.; 1972: *SHAKE: a computer program for earthquake response analysis of horizontally layered sites*. Earthquake Engineering Research Center, Report No. UCB/EERC-72/12, University of California, Berkeley, 102 pp.

Seed H.B. and Idriss I.M.; 1970: *Soil moduli and damping factors for dynamic response analysis*. Earthquake Engineering Research Center, Report No. UCB/EERC- 70/10, University of California, Berkeley, 48 pp.

Seed H.B., Wong R.T., Idriss I.M. and Tokimatsu K.; 1986: *Moduli and damping factors for dynamic analyses of cohesionless soils*. Journal of the Geotechnical Engineering Division, **112**, 1016-1032.

Slejko D., Peruzza L. and Rebez A.; 1998: *Seismic Hazard maps of Italy*. Annali di Geofisica, **41**, 183-214.

Sun J. I., Golesorkhi R. and Seed H. B.; 1988: *Dynamic moduli and damping ratios for cohesive soils*. Earthquake Engineering Research Center, Report No. UCB/EERC-88/15, University of California, Berkeley, 42 pp.

Wills C.J., Petersen M., Bryant W.A., Reichle M., Saucedo G.J., Tan S., Taylor G. and Treiman J.; 2000: *A site-condition map for California based on geology and shear- wave velocity*. Bull. Seism. Soc. Am., **90**, S187-S208.

Corresponding author: Daniela Di Bucci
Presidenza del Consiglio dei Ministri, Dipartimento della Protezione Civile
Servizio Sismico Nazionale, Via Vitorchiano 4, 00189 Roma, Italy
phone: +39 06 68204761; fax: +39 06 68202877; e-mail: daniela.dibucci@protezionecivile.it